AIAA JOURNAL
Vol. 42, No. 6, June 2004

Mixed Analytical/Numerical Method for Low-Reynolds-Number k–ε Turbulence Models

Tao Du* and Zi-Niu Wu†
Tsinghua University, 100084 Beijing, People's Republic of China

The mixed analytical/numerical method previously proposed for solving partial differential equations with an oscillating source term is extended to solve low-Reynolds-number k–ε turbulent models. The convection–diffusion part is solved by a traditional numerical scheme and the source term by an analytical method. The analytical solution is obtained when the damping functions, due to low-Reynolds-number effect, are frozen to be constant at each time step. Several standard test cases are used to demonstrate that the mixed method is more stable and converges faster than the traditional method.

Nomenclature

A	=	Jacobian of the source term
a	=	speed of sound
$C_{\varepsilon 1}, C_{\varepsilon 2}, C_\mu, \sigma_k, \sigma_\varepsilon$	=	model constants defined in Table 1
D, E_k, E_ε	=	damping functions defined in Table 3
E	=	total energy
f_1, f_2, T_l, f_μ	=	damping factors defined in Table 2
k	=	turbulent kinetic energy
M	=	Mach number
P_k	=	production term, $= C_\mu(\kappa^2/\varepsilon)\Phi$
p	=	static pressure
$\boldsymbol{q}$	=	heat flux vector
R	=	the space discretization part for Navier–Stokes equation
Re	=	Reynolds number
S	=	source term
S_D	=	source term due to the additional damping terms
S_s	=	standard part source term
T	=	temperature
$\boldsymbol{U}$	=	unknown vector of the Navier–Stokes equations
$\boldsymbol{U}_j$	=	component of the mean velocity vector
$\boldsymbol{U}^T$	=	unknown vector for the turbulent model equation
u, v	=	x-, y-wise velocity components
γ	=	ratio of specific heat, 1.4
Δt	=	time step
δ_{ij}	=	Kronecker tensor
ε	=	turbulent dissipation rate
$\tilde{\varepsilon}$	=	corrected dissipation rate
μ	=	molecular viscosity
μ_t	=	turbulent eddy viscosity
ρ	=	density
σ	=	stress tensor
Φ	=	product of strain rate tensor

Subscripts

k	=	term for turbulent kinetic energy equation
T	=	turbulence
ε	=	term for turbulent dissipation rate equation
0	=	initial condition
∞	=	freestream condition

Superscripts

(m)	=	level in multistage scheme
n	=	time level
$-$	=	negative part

Received 14 May 2003; revision received 27 November 2003; accepted for publication 13 January 2004.

*Ph.D Student, Department of Engineering Mechanics.
†Professor, Department of Engineering Mechanics; ziniuwu@tsinghua.edu.cn.

I. Introduction

THE k–ε turbulence model is widely used for the solution of turbulent flows in engineering applications. The major drawback of the original k–ε model is probably the near-wall formulation, which fails to reproduce correctly the effects of the solid boundary on turbulence. There are two methods available to repair this trouble: wall function method and low-Reynolds-number correction. Launder[1] indicated that the application of the second method in the near-wall region caused a marked improvement over the first approach in the prediction of the local heat transfer coefficients. In the past, various forms of low-Reynolds-number k–ε turbulent models have been proposed.[2–5] The detail of two-equation models and low Reynolds corrections are presented in Ref. 6.

Though mathematically the k–ε model is well posed,[7] the strong nonlinearities may interact with numerical errors in such a way that computation may break down easily. A typical behavior of unstable computations involves the loss of positivity of k or ε, though the original differential equations have positive solution. (See Ref. 8 for more details of positivity analysis.) The appearance of negative values changes the sign of several terms in the models, so that turbulent quantities may increase unboundedly.[9] Even though the two turbulence equations can be solved in exactly the same manner as for the mean flow equations, it has been found that such a method often leads to an unstable solution, or even incorrect solutions.[10] In general, both the advection–diffusion part and the source term must be considered to determine the time step. Sometimes, especially for low Reynold turbulent model, the latter restricts the time step more severely.[10,11] The damping functions in the low Reynolds turbulent models improve the model prediction capability for near-wall flow, but also introduce more severe numerical stiffness for the source terms.

There are a huge amount of numerical methods for compressible Navier–Stokes equations coupled with two equation models. Vandromme and Ha Minh[12] applied an implicit scheme to the mean and turbulent equations, which is solved fully coupled. Sahu and Danberg[13] solved the mean and turbulent equations decoupled with the source terms treated implicitly but as part of one of the spatial factors. Shih and Chyu[14] recommended the inclusion of the source

terms in the spatial factors rather as a separate inversion to reduce factorization error. Huang and Coakley[15] split the source terms, on a term-by-term basis, into positive and negative parts, with the positive source treated explicitly and the negative source treated implicitly. A recent account for efficient treatment of source terms in two-equation turbulence models is given in Ref. 16. Kunz and Lakshminarayana[17] investigated the stability of explicit for k–ε turbulent model and concluded that the k/ε term may be responsible for near-wall instabilities in low-Reynolds-number models.

The two-equation turbulent model is a typical example of partial differential equations with source terms. Great progress has been made in efficient treatment of the source terms.[18–21] Helzel et al.[22] treated chemically reacting flow with an Arrhenius law for the source term by mixed method in detonation waves computation. In Ref. 23, a mixed analytical/numerical method for oscillating source terms is studied. In this method, the advection–diffusion part and the source terms are treated separately through operator splitting. The advection–diffusion part [partial differential equations (PDE)] is integrated numerically, whereas the source term part [ordinary differential equations (ODE)] is integrated analytically. Hence, this method is called mixed analytical/numerical. The mixed method performs well for PDEs with source terms, in which the source term timescale is much smaller than the mean flow scale inherent to the advection–diffusion part. Later, the authors extended the mixed method to the implicit solution of high-Reynolds-number compressible turbulent flows.[24] Numerical results show that the mixed method can give robust, steady, and fast convergence solutions.

In this paper, we extend the mixed method to low-Reynold-number turbulent models. The essential new feature of the mixed method for low-Reynolds-number turbulent models lies in the treatment of the source terms that contain new damping functions. With respect to the high-Reynolds-number counterpart, the low-Reynolds-number turbulent models retain the original source terms modified with damping factors and sometimes contain additional damping terms. In the mixed method proposed in this paper, the damping factors are treated as constant at each time step, so that the main part of the source terms are still analytically integrable at each time step. The additional damping terms are treated numerically.

To assess the new method, we calculate numerous standard test cases, including the transonic diffuser problem, RAE2822 airfoil problem, and so on by using the Jones–Launder model,[2] the Launder–Sharma model,[3] the Lam–Bremhorst model,[25] the wall-distance-free Goldberg-Apsley model,[4] and the Hwang–Lin model.[5]

The rest of the paper is organized as follows. In Sec. II, the governing equations of Navier–Stokes equations with various low Reynolds k–ε turbulent models and the numerical method are briefly outlined. In Sec. III, the mixed method for low Reynolds k–ε turbulent model is discussed. A mixed method based on unsplit method is suggested. In Sec. IV, numerical results are provided. Concluding remarks are given at the end of the paper.

II. Governing Equations and Turbulence Models

A. Governing Equations

The governing equations are obtained by Favre averaging the Navier–Stokes equations and modeling the Reynolds stress. In conservative form, these equations, restricted to dimensions in this study, are written as

$$\frac{\partial \boldsymbol{U}}{\partial t}+\frac{\partial F_c}{\partial x}+\frac{\partial G_c}{\partial y}=\frac{\partial F_v}{\partial x}+\frac{\partial G_v}{\partial y}+S \tag{1}$$

with

$$U=\begin{pmatrix}\rho\\ \rho u\\ \rho v\\ \rho E\\ \rho k\\ \rho\tilde{\varepsilon}\end{pmatrix},\qquad F_c=\begin{pmatrix}\rho u\\ \rho u^2+p\\ \rho uv\\ (\rho E+p)u\\ \rho uk\\ \rho u\tilde{\varepsilon}\end{pmatrix}$$

$$G_c=\begin{pmatrix}\rho v\\ \rho vu\\ \rho v^2+p\\ (\rho E+p)v\\ \rho vk\\ \rho v\tilde{\varepsilon}\end{pmatrix} \tag{2}$$

$$S=\begin{pmatrix}0\\ 0\\ 0\\ 0\\ \mu_t P_k-\rho\tilde{\varepsilon}+E_k\\ (f_1C_{\varepsilon 1}P_k-f_2C_{\varepsilon 2}\rho\tilde{\varepsilon})\,T_l^{-1}+E_\varepsilon\end{pmatrix} \tag{3}$$

and, for a perfect gas, $p=(\gamma-1)\rho[E-\frac{1}{2}(u^2+v^2)]$. Here $\tilde{\varepsilon}$ is related to ε through $\tilde{\varepsilon}=\varepsilon-D$. The viscous flux are defined by

$$F_v=\begin{pmatrix}0\\ \sigma_{xx}\\ \sigma_{xy}\\ u\sigma_{xx}+v\sigma_{xy}-\boldsymbol{q}_x\\ \left(\mu+\dfrac{\mu_t}{\sigma_k}\right)\dfrac{\partial k}{\partial x}\\ \left(\mu+\dfrac{\mu_t}{\sigma_\varepsilon}\right)\dfrac{\partial\tilde{\varepsilon}}{\partial x}\end{pmatrix},\qquad G_v=\begin{pmatrix}0\\ \sigma_{yx}\\ \sigma_{yy}\\ u\sigma_{yx}+v\sigma_{yy}-\boldsymbol{q}_y\\ \left(\mu+\dfrac{\mu_t}{\sigma_k}\right)\dfrac{\partial k}{\partial x}\\ \left(\mu+\dfrac{\mu_t}{\sigma_\varepsilon}\right)\dfrac{\partial\tilde{\varepsilon}}{\partial x}\end{pmatrix} \tag{4}$$

where σ represents the stress tensor and $\boldsymbol{q}$ the heat flux vector, which are given by

$$\sigma_{xx}=2(\mu+\mu_t)\frac{\partial u}{\partial x}-\frac{2}{3}(\mu+\mu_t)\left(\frac{\partial u}{\partial x}+\frac{\partial v}{\partial y}\right)-\frac{2}{3}\rho k \tag{5}$$

$$\sigma_{yy}=2(\mu+\mu_t)\frac{\partial v}{\partial y}-\frac{2}{3}(\mu+\mu_t)\left(\frac{\partial u}{\partial x}+\frac{\partial v}{\partial y}\right)-\frac{2}{3}\rho k \tag{6}$$

$$\sigma_{xy}=\sigma_{yx}=(\mu+\mu_t)\left(\frac{\partial u}{\partial x}+\frac{\partial v}{\partial y}\right) \tag{7}$$

$$\boldsymbol{q}_x=-\frac{\gamma}{\gamma-1}\left(\frac{\mu}{Pr}+\frac{\mu_t}{Pr_t}\right)\frac{\partial(p/\rho)}{\partial x} \tag{8}$$

$$\boldsymbol{q}_y=-\frac{\gamma}{\gamma-1}\left(\frac{\mu}{Pr}+\frac{\mu_t}{Pr_t}\right)\frac{\partial(p/\rho)}{\partial y} \tag{9}$$

Here, Pr is the laminar Prandtl number, which is taken as 0.7 for air. Pr_t is the turbulent Prandtl number, taken as 0.9. The molecule dynamic viscosity μ is assumed to be a function of the temperature, following the well-known Sutherland's law.

In the source term S, the turbulence production term is

$$P_k=\mu_t\left[\left(\frac{\partial \boldsymbol{U}_i}{\partial x_j}+\frac{\partial \boldsymbol{U}_j}{\partial x_i}-\frac{2}{3}\frac{\partial \boldsymbol{U}_l}{\partial x_l}\delta_{ij}\right)-\frac{2}{3}\rho k\delta_{ij}\right]\frac{\partial U_i}{\partial x_j} \tag{10}$$

The eddy viscosity is calculated as

$$\mu_t=f_\mu C_\mu\rho k^2\big/\tilde{\varepsilon} \tag{11}$$

The damping functions f_1, f_2, E_k, T_l, and E_ε depend on the specific choice of low-Reynolds-number turbulence models and are given in the next subsection.

B. Turbulence Model

Five models will be used in this paper. These include, 1) the Jones–Launder (JL) model,[2] 2) the Launder–Sharma (LS) model[3] with Yap correction,[26] 3) the Lam–Bremhorst (LB) model,[25] 4) the wall-distance-free Goldberg–Apsley (GA) model,[4] and 5) the Hwang–Lin (HL) model.[5]

Models 2 and 3 are actually extensions of the JL model, which have been introduced to improve some of the drawbacks of the standard k–ε model, primarily the numerical stiffness associated with the source terms. The GA model is the recently developed k–ε model based on a wall-distance-free formulation. The HL model is based on the near-wall characteristic obtained with direct numerical simulation data. Let $y_\lambda = y/\sqrt{(\nu k/\tilde{\varepsilon})}$, $R_t \equiv k^2/(\nu\tilde{\varepsilon})$, $R_y = \sqrt{(k)}y/\nu$, $\xi \equiv \sqrt{(R_t)}/C_\tau$, $C_\tau = \sqrt{2}$, $S = \sqrt{(2S_{i,j}S_{i,j})}$, $S_{i,j} = (\boldsymbol{U}_{i,j} + \boldsymbol{U}_{i,i})/2$, $\Pi = \boldsymbol{U}_i\boldsymbol{U}_i/2 + k$, $A_k = 0.05$, $A_\mu = 0.01$, and $A_f = 0.231$. The damping functions appearing in source term (3) are summarized in Tables 1–3.

C. Basic Numerical Method for Traditional Treatment

1. Time Advancing Method for the Navier–Stokes Equations

Let $R(\boldsymbol{U}^n)$ represent the contribution from the space discretization of the Navier–Stokes equations plus the turbulence models. To advance the solution in time, we use a simplified four-stage Runge–Kutta scheme (see Ref. 27) as defined by

$$\begin{aligned} \boldsymbol{U}^{(0)} &= \boldsymbol{U}^n \\ \boldsymbol{U}^{(i)} &= \boldsymbol{U}^{(0)} + \alpha_i \Delta t R\left(\boldsymbol{U}^{(i-1)}\right), \qquad i = 1, \ldots, 4 \\ \boldsymbol{U}^{n+1} &= \boldsymbol{U}^{(4)} \end{aligned} \tag{12}$$

with $\{\alpha_1, \alpha_2, \alpha_3, \alpha_4\} = \{\frac{1}{4}, \frac{1}{3}, \frac{1}{2}, 1\}$.

The time step is determined by

$$\Delta t = \frac{\mathrm{CFL}}{|\nabla\xi|t_1 + |\nabla\eta|t_2} \tag{13}$$

$$t_1 = |\bar{U}| + a + 2|\nabla\xi|(\mu + \mu_T)\max\left(\frac{4}{3}, \frac{\gamma}{Pr}\right)\frac{Ma}{\mathrm{Re}}\frac{1}{\rho}$$

$$t_2 = |\bar{V}| + a + 2|\nabla\eta|(\mu + \mu_T)\max\left(\frac{4}{3}, \frac{\gamma}{Pr}\right)\frac{Ma}{\mathrm{Re}}\frac{1}{\rho}$$

For the scheme to be stable, the Courant–Friedrichs–Lewy (CFL) number is usually bounded from a value of order of unity. Local time stepping is used to accelerate convergence for steady-state computation. For the transonic diffuser, an implicit residual smoothing technique will be used to test the stability for large time steps. This will be made clearer when the numerical results are presented.

2. Space Discretization

The viscous part of the space terms is discretized with second-order central differences, whereas the inviscid part is approximated by the Roe's scheme[28] combined with the MUSCL treatment[29] to achieve second-order accuracy. Limiters may be used to eliminate spurious wiggles at discontinuities.[30]

3. Traditional Implicit and Explicit Treatment of the Turbulence Model

The advection–diffusion part of the two-equation model is discretized in the same way as the Navier–Stokes equations. Only the source term needs special treatment. The fundamental means is to

Table 1 Closure coefficients for turbulence model

Model	$C_{\varepsilon 1}$	$C_{\varepsilon 2}$	C_μ	σ_k	σ_ε
JL	1.55	2.00	0.09	1.0	1.3
LS	1.44	1.92	0.09	1.0	1.3
LB	1.44	1.92	0.09	1.0	1.3
GA	1.42	1.83	0.09	1.367	1.367
HL	1.44	1.92	0.09	1.4–1.1 $\exp[-(y_\lambda/10)]$	1.3–1.0 $\exp[-(y_\lambda/10)]$

Table 2 Damping function for various models 1

Model	f_1	f_2	T_l	f_μ
JL	1	$1 - 0.3\exp\left(-\mathrm{Re}_t^2\right)$	$\frac{k}{\tilde{\varepsilon}}$	$\exp\frac{-2.5}{(1+\mathrm{Re}_T/50)^2}$
LS	1	$1 - 0.3\exp\left(-\mathrm{Re}_t^2\right)$	$\frac{k}{\tilde{\varepsilon}}$	$\exp\frac{-3.4}{(1+\mathrm{Re}_T/50)^2}$
LB	$1 + \left(\frac{0.05}{f_\mu}\right)^3$	$1 - \exp\left(-\mathrm{Re}_t^2\right)$	$\frac{k}{\tilde{\varepsilon}}$	$\frac{[1-\exp(-0.0165R_y)]^2}{(1+20.5/\mathrm{Re}_T)^{-1}}$
GA	1	1	$\frac{k}{\tilde{\varepsilon}}\max\{1, \xi^{-1}\}$	$\frac{1-\exp(-A_\mu R_t)}{1-\exp\left(-\sqrt{R_t}\right)}\max\{1, \xi^{-1}\}$
HL	1	1	$\frac{k}{\tilde{\varepsilon}}$	$1 - \exp\left(-0.01y_\lambda - 0.008y_\lambda^3\right)$

Table 3 Damping function for various models 2

Model	D	E_k	E_ε
JL	$2\nu\left(\frac{\partial\sqrt{k}}{\partial n}\right)^2$	$2\nu\left(\frac{\partial\sqrt{k}}{\partial x_k}\right)^2$	$2\nu\nu_T\left(\frac{\partial^2 U}{\partial x_k \partial x_l}\right)^2$
LS	$2\nu\left(\frac{\partial\sqrt{k}}{\partial n}\right)^2$	$2\nu\left(\frac{\partial\sqrt{k}}{\partial x_k}\right)^2$	$2\nu\nu_T\left(\frac{\partial^2 U}{\partial x_k \partial x_l}\right)^2 + YC$[a]
LB	0	0	0
GA	0	0	$\frac{2A_kC_2}{C_\tau A_\mu}\mu f_\mu S^2\exp\left(-A_f\sqrt{\Pi/\nu S}\right)$
HL	$2\nu\left(\frac{\partial\sqrt{k}}{\partial n}\right)^2$	$2\nu\left(\frac{\partial\sqrt{k}}{\partial x_k}\right)^2 - \frac{1}{2}\frac{\partial}{\partial x_j}\left(\nu\frac{k}{\varepsilon}\frac{\partial D}{\partial x_j}\right)$	$-\frac{1}{2}\frac{\partial}{\partial x_j}\left(\nu\frac{\tilde{\varepsilon}}{k}\frac{\partial k}{\partial x_j}\right)$

[a]Term YC is a correction as proposed by Yap[26] for reducing the unrealistic level of near-wall turbulence in separated flows.

treat the negative source terms implicitly and the positive terms explicitly.[12,16] However, the time step still has to be small enough to obtain realistic values of k, ε, and μ_t. The naïve use of the local time-step size determined for the mean flow Navier–Stokes equations will lead to unrealistic values of k and ε and instability.[10]

Similar to scheme (12) for the Navier–Stokes equations, the turbulence model is approximated by the following scheme, which differs from Eq. (12) only through the occurrence of a source term,

$$[(1/\Delta t)I - A^n]\Delta(\boldsymbol{U}^T)^n = R^T[(\boldsymbol{U}^T)^n] + S[(\boldsymbol{U}^T)^n] \tag{14}$$

where the superscript T means turbulence. Matrix A is the Jacobian of some part of the source term.

According to Ref. 15, the different terms of Eq. (14) are better treated implicitly for the negative part and explicitly for the positive

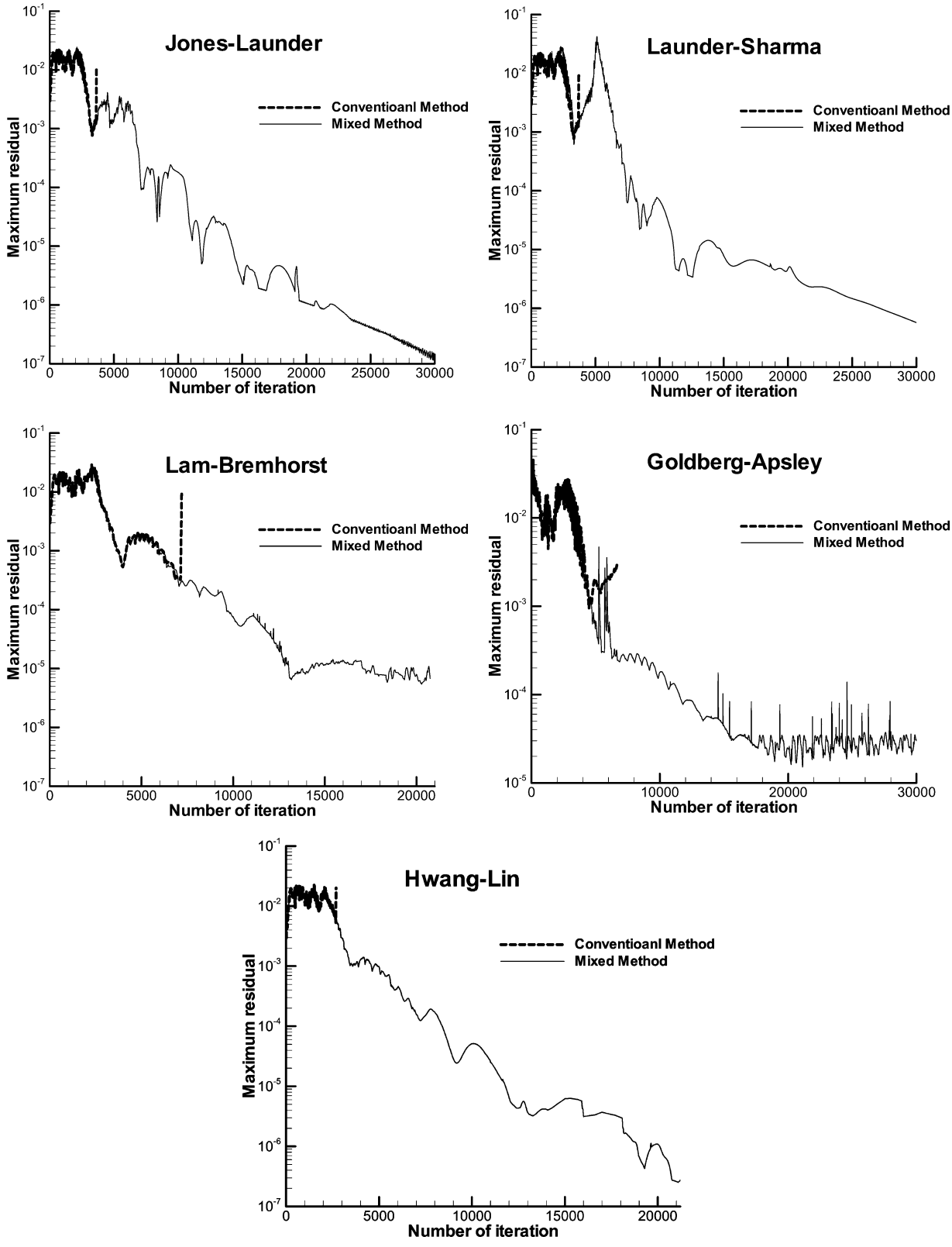

Fig. 1 Convergence history for transonic diffuser: mixed method and traditional method.

part, so that A is defined by

$$A = \frac{\partial S^-}{\partial \boldsymbol{U}^T}$$

In the point-implicit method of Ref. 12, A is defined by

$$A = [S^-/\boldsymbol{U}^T]^n \tag{15}$$

In the approximate Jacobian method of Ref. 31, A is first defined by

$$A = \frac{\partial S^-}{\partial \boldsymbol{U}^T} = \begin{bmatrix} \dfrac{\partial S_k^-}{\partial k} & \dfrac{\partial S_k^-}{\partial \varepsilon} \\ \dfrac{\partial S_\varepsilon^-}{\partial k} & \dfrac{\partial S_\varepsilon^-}{\partial \varepsilon} \end{bmatrix} \tag{16}$$

and then replaced by its diagonal counterpart to simplify the inversion:

$$A = \begin{bmatrix} \dfrac{2C_\mu \rho k}{\mu_t} & 0 \\ 0 & \dfrac{3}{2}C_{\mu 2}\sqrt{\dfrac{C_\mu \rho \varepsilon}{\mu_t}} \end{bmatrix} \tag{17}$$

III. Mixed Analytical/Numerical Method for Low-Reynolds-Number Turbulent Models

The turbulence model equations contain advection–diffusion operators and source terms. In the conventional treatment just presented, both the advection–diffusion operators and the source terms are integrated numerically. In the mixed analytical/numerical method, the advection–diffusion part (PDE) is integrated numerically as usual, whereas the source term (ODE) is integrated analytically.

A. Treatment of the Source Terms

The analytical solution of the source terms for high-Reynolds-number turbulence models is given in Reference.[23] With respect to the high-Reynolds-number counterpart, the low-Reynolds-number turbulent models retain the original source terms modified with damping factors and sometimes contain additional damping terms. In the mixed method proposed in this paper, the damping factors are frozen as constant at each time step, so that the main part of the source terms are still analytically integrable at each time step. The additional damping terms are treated numerically.

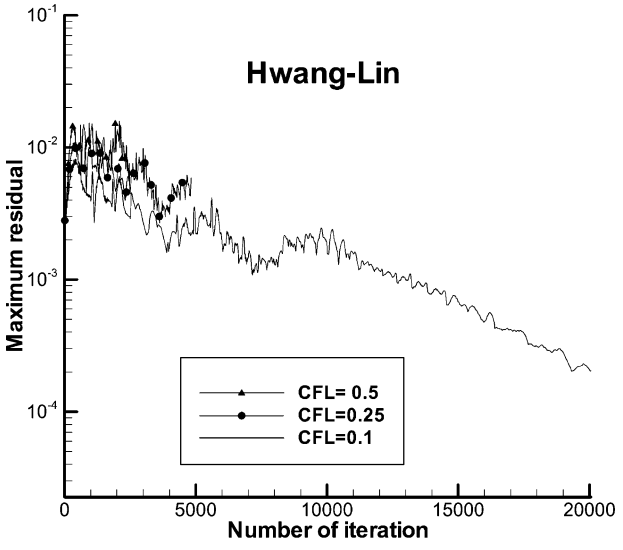

Fig. 2 Convergce history of conventional method for HL model with various CFL numbers.

Following the original construction of the mixed method, we first consider the ODE due to the source terms:

$$\frac{\mathrm{d}\boldsymbol{U}^T}{\mathrm{d}t} = S_s(\boldsymbol{U}) + S_D(\boldsymbol{U}) \tag{18}$$

Here, $S_s(\boldsymbol{U})$ is the standard part, which is similar to the source term of the high-Reynolds-number model, modified only by the addition of damping factors, and $S_D(\boldsymbol{U})$ stands for the additional damping terms. Precisely, $S_s(\boldsymbol{U})$ is defined by

$$S_s(\boldsymbol{U}) = \begin{pmatrix} P_k - \rho\tilde{\varepsilon} \\ f_1 C_{\varepsilon 1}\dfrac{\tilde{\varepsilon}}{k}P_k - f_2 C_{\varepsilon 2}\dfrac{\rho\tilde{\varepsilon}^2}{k} \end{pmatrix} \tag{19}$$

The additional damping terms $S_D(\boldsymbol{U})$ are treated numerically, whereas the standard part $S_s(\boldsymbol{U})$ is solved analytically by consideration of the following ODE:

$$\frac{\mathrm{d}\rho k}{\mathrm{d}t} = P_k - \rho\tilde{\varepsilon}, \qquad \frac{\mathrm{d}\rho\tilde{\varepsilon}}{\mathrm{d}t} = C'_{\varepsilon 1}\frac{\tilde{\varepsilon}}{k}P_k - C'_{\varepsilon 2}\frac{\rho\tilde{\varepsilon}^2}{k} \tag{20}$$

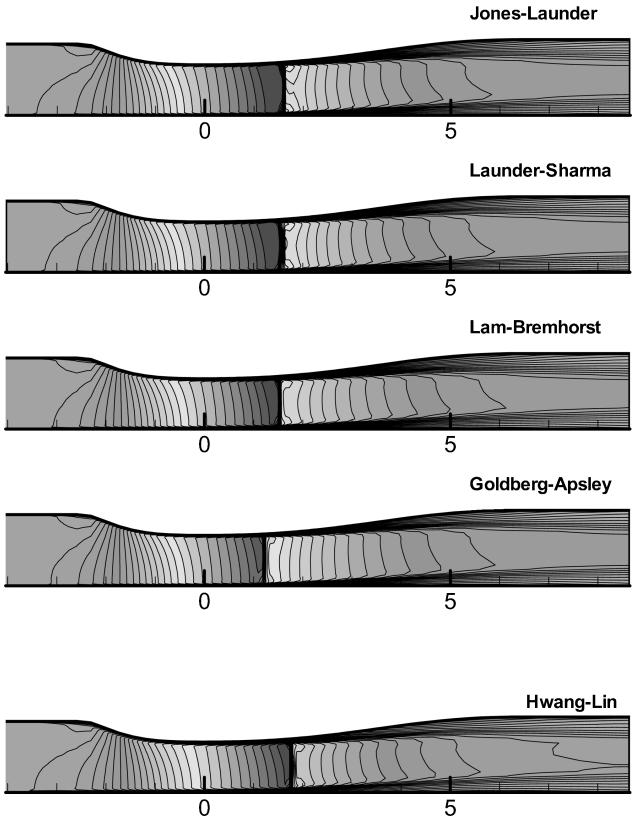

Fig. 3 Mach contour of transonic diffuser for $R = 0.82$ (weak shock).

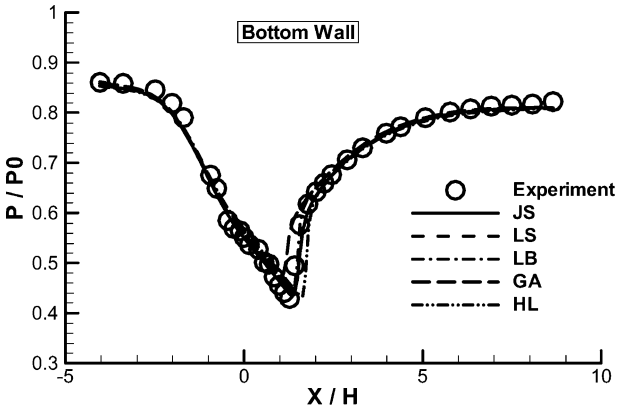

Fig. 4 Static pressure distribution along bottom wall.

with the parameters

$$C'_{\varepsilon 1} = f_1 C_{\varepsilon 1}, \qquad C'_{\varepsilon 2} = f_2 C_{\varepsilon 2}, \qquad C'_{\mu} = f_\mu C_\mu \tag{21}$$

treated as constant at each time step. Hence, the standard part should have the same form of analytical solution as the high-Reynolds-number model.

To find the analytical solution of Eq. (20), we rewrite it as

$$\frac{\mathrm{d}k}{\mathrm{d}t} = \nu_T \Phi - \tilde{\varepsilon}, \qquad \frac{\mathrm{d}\tilde{\varepsilon}}{\mathrm{d}t} = C'_{\varepsilon 1} \nu_T \frac{\tilde{\varepsilon}}{k} \Phi - C'_{\varepsilon 2} \frac{\tilde{\varepsilon}^2}{k} \tag{22}$$

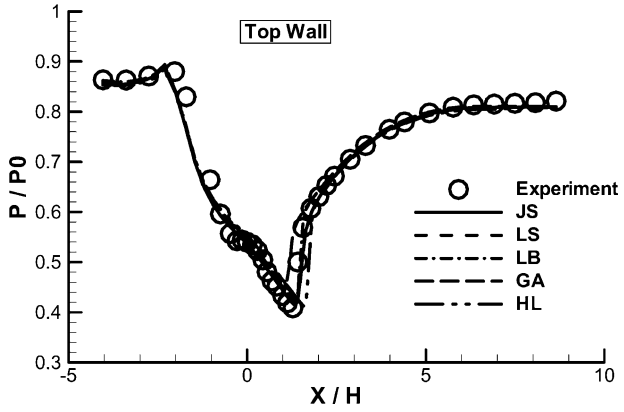

Fig. 5 Static pressure distribution along top wall.

where $\Phi = P_k/\mu_T$. Set $\theta = k/\tilde{\varepsilon}$, then we can rewrite Eq. (22) as

$$\frac{\mathrm{d}\,\ell n\, k}{\mathrm{d}t} = C'_{\mu} \Phi \theta - \frac{1}{\theta}, \qquad \frac{\mathrm{d}\,\ell n\, \varepsilon}{\mathrm{d}t} = C'_{\varepsilon 1} C'_{\mu} \Phi \theta - C'_{\varepsilon 2} \frac{1}{\theta} \tag{23}$$

By combining the two Eqs. (22), we obtain

$$\frac{\mathrm{d}\theta}{\mathrm{d}t} = b^2 (a^2 - \theta^2) \tag{24}$$

with

$$a = \sqrt{\frac{C'_{\varepsilon 2} - 1}{\Phi C'_{\mu} (C'_{\varepsilon 1} - 1)}}, \qquad b = \sqrt{\Phi C'_{\mu} (C'_{\varepsilon 1} - 1)}$$

Because we have frozen the damping functions at each time step, the parameter a and b can be considered as constant at each time step. Within each time step, the solution of Eq. (24) is found to be

$$\theta = -\varrho \Phi^{-\frac{1}{2}} \frac{(\Psi_0 - \varrho) + (\Psi_0 + \varrho) \exp\left(2\varkappa \Phi^{\frac{1}{2}} t\right)}{(\Psi_0 - \varrho) - (\Psi_0 + \varrho) \exp\left(2\varkappa \Phi^{\frac{1}{2}} t\right)} \tag{25}$$

where

$$\varkappa = b^2 a \Phi^{-\frac{1}{2}}, \qquad \varrho = a \Phi^{\frac{1}{2}}, \qquad \Psi_0 = (\kappa_0/\varepsilon_0) \Phi^{\frac{1}{2}}$$

Inserting Eq. (25) into Eqs. (23), we obtain a self-contained equation for k and a self-contained equation for $\tilde{\varepsilon}$, which can then be

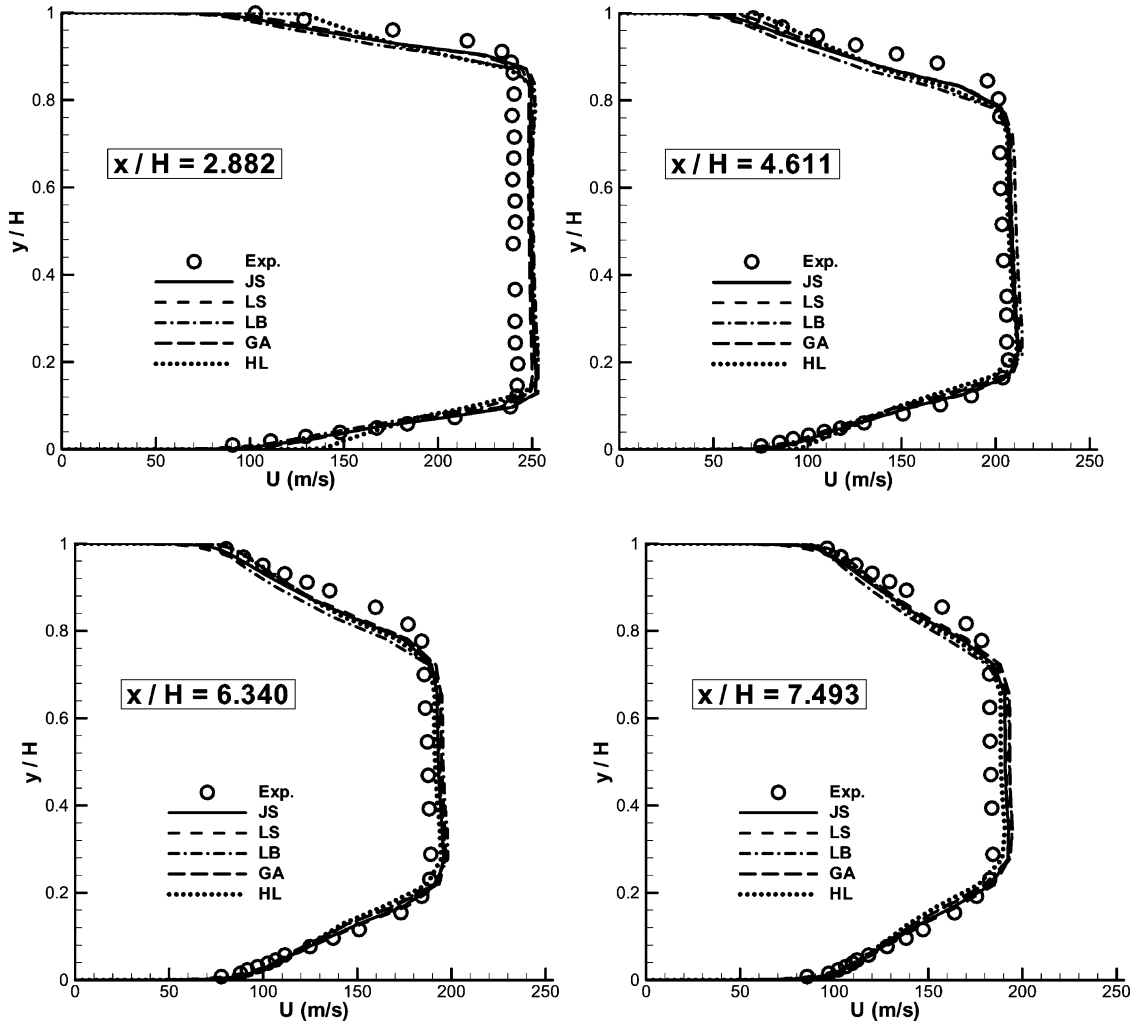

Fig. 6 Velocity profiles at four axial locations for the Sajben–Kroutil diffuser: numerical results obtained with mixed method.

integrated to yield

$$\rho k = K[(\rho k)_0, (\rho\tilde{\varepsilon})_0, t]$$

$$= (\rho k)_0 2^{\alpha} F^{\gamma} [G/(1/\rho)\Psi_0]^{-\beta} \exp\left(-\varkappa\sqrt{\Phi}t\right) \tag{26}$$

$$\rho\tilde{\varepsilon} = L[(\rho k)_0, (\rho\tilde{\varepsilon})_0, t]$$

$$= (\rho\tilde{\varepsilon})_0 2^{\alpha} F^{\nu} [G/(1/\rho)\Psi_0]^{-\tau} \exp\left(-\varkappa\sqrt{\Phi}t\right) \tag{27}$$

where $\Psi_0 = \Phi^{(1/2)k_0}/\tilde{\varepsilon}_0$,

$$F = 1 - \frac{1}{\varrho}\Psi_0 + \left(1 + \frac{1}{\varrho}\Psi_0\right) e^{2\varkappa\sqrt{\Phi}t}$$

$$G = \frac{1}{\varrho}\Psi_0 - 1 + \left(1 + \frac{1}{\varrho}\Psi_0\right) e^{2\varkappa\sqrt{\Phi}t}$$

$$\varkappa = \sqrt{(C'_{\varepsilon 2} - 1)C'_{\mu}(C'_{\varepsilon 1} - 1)}, \qquad \varrho = \sqrt{\frac{(C'_{\varepsilon 2} - 1)}{[C'_{\mu}(C'_{\varepsilon 1} - 1)]}}$$

$$\alpha = \frac{1 - C'_{\mu}\varrho^2}{\varkappa\varrho} = \frac{C'_{\varepsilon 1} - C'_{\varepsilon 2}}{(C'_{\varepsilon 1} - 1)(C'_{\varepsilon 2} - 1)}$$

$$\beta = \frac{1}{\varkappa\varrho} = \frac{1}{C'_{\varepsilon 2} - 1}$$

$$\zeta = \frac{C'_{\mu}\varrho}{\varkappa} = \frac{1}{C'_{\varepsilon 1} - 1}$$

$$\varkappa = \frac{C'_{\mu}\varrho^2 - 1}{\varrho} = \frac{C'_{\mu}(C'_{\varepsilon 2} - C'_{\varepsilon 1})}{\sqrt{[(C'_{\varepsilon 2} - 1)C'_{\mu}(C'_{\varepsilon 1} - 1)]}}$$

$$\varsigma = \frac{C'_{\varepsilon 2} - C'_{\varepsilon 1}C'_{\mu}\varrho^2}{\varkappa\varrho} = \frac{C'_{\varepsilon 1} - C'_{\varepsilon 2}}{(C'_{\varepsilon 1} - 1)(C'_{\varepsilon 2} - 1)}$$

$$\varpi = \frac{C'_{\varepsilon 2}}{\varkappa\varrho} = \frac{C'_{\varepsilon 2}}{C'_{\varepsilon 2} - 1}$$

$$\upsilon = \frac{C'_{\varepsilon 1}C'_{\mu}\varrho}{\varkappa} = \frac{C'_{\varepsilon 1}}{C'_{\varepsilon 1} - 1}$$

$$\sigma = \frac{C'_{\varepsilon 1}C'_{\mu}\varrho^2 - C'_{\varepsilon 2}}{\varrho} = \frac{C'_{\mu}(C'_{\varepsilon 2} - C'_{\varepsilon 1})}{\sqrt{[(C'_{\varepsilon 2} - 1)C'_{\mu}(C'_{\varepsilon 1} - 1)]}}$$

Here, k_0 and $\tilde{\varepsilon}_0$ stand for initial value of turbulent kinetic energy k and dissipation rate $\tilde{\varepsilon}$.

B. Mixed Analytical/Numerical Method

The mixed method for low-Reynolds-number models can be written as

$$[(1/\Delta t)I - A^n]\Delta(\boldsymbol{U}^T)^n = R^T[(\boldsymbol{U}^T)^n] + \overline{S_s}[(\boldsymbol{U}^T)^n] + S_D[(\boldsymbol{U}^T)^n] \tag{28}$$

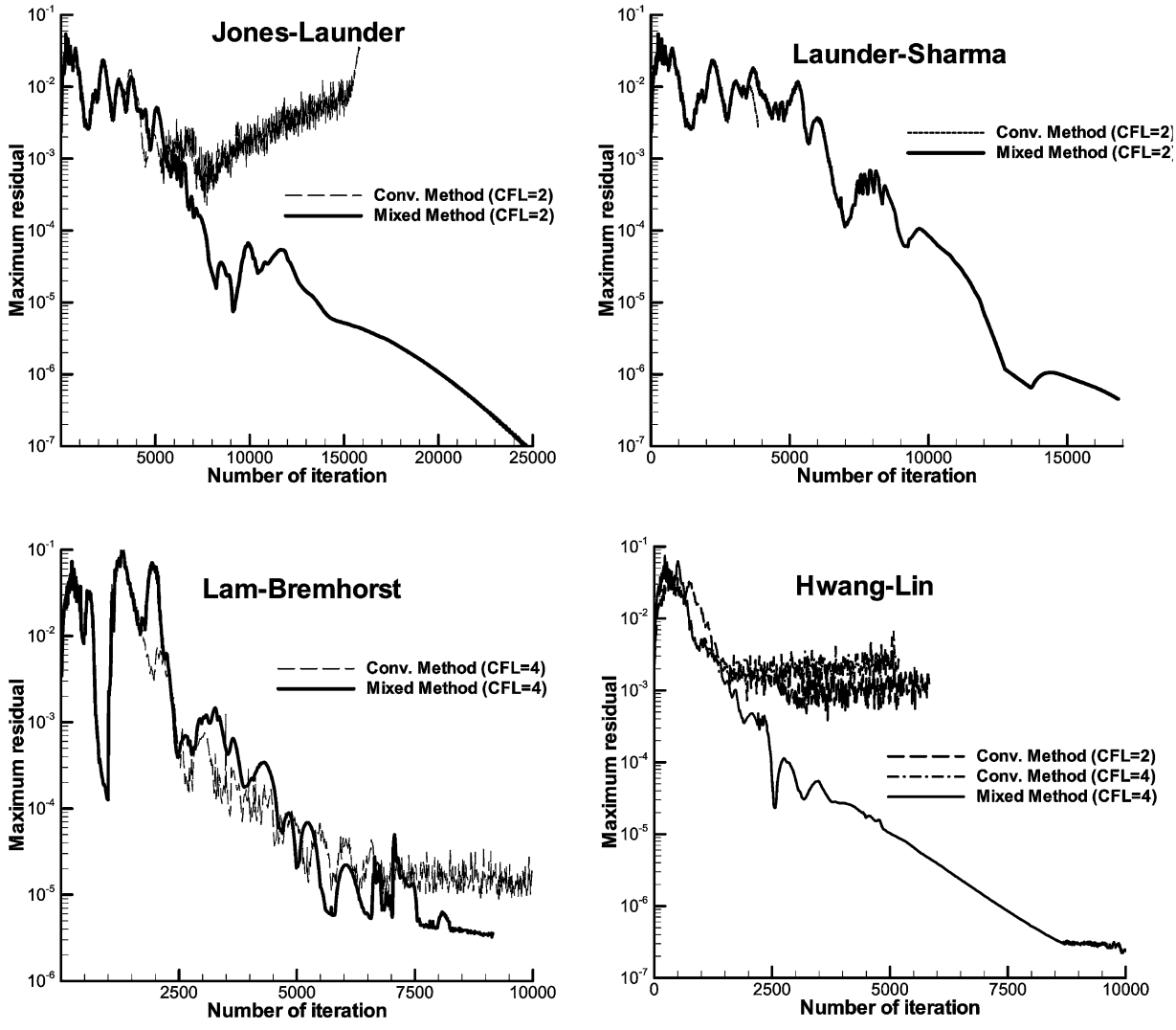

Fig. 7 Convergence history for transonic diffuser: mixed method and traditional method with IRS.

where $\overline{S_s}[(\boldsymbol{U}^T)^n]$ is the analytical solution to the standard part, as defined by

$$\overline{S_s}[(\boldsymbol{U}^T)^n] = \frac{1}{\Delta t}\begin{bmatrix} K[(\rho k)^n, (\rho\tilde{\varepsilon})^n, \Delta t] - (\rho k)^n \\ L[(\rho k)^n, (\rho\tilde{\varepsilon})^n, \Delta t] - (\rho\tilde{\varepsilon})^n \end{bmatrix} \tag{29}$$

Here, $K(k^n, \tilde{\varepsilon}^n, \Delta t)$ and $L(k^n, \tilde{\varepsilon}^n, \Delta t)$ are defined by Eqs. (26) and (27), respectively, and $S_D[(\boldsymbol{U}^T)^n]$ is due to the additional damping terms integrated by the use of the same time advancing scheme as that used for the advection–diffusion part.

The turbulence models sometimes produce unrealistic large values of k or $\tilde{\varepsilon}$ (Ref. 24), and cause unrealistically large values of turbulent kinetic energy and eddy viscosity in stagnation regions.[32] Hence, a limiter is required as for any numerical methods. In the present paper, we use Menter's limiter[33] in Eq. (29), which restricts the production term for the k equation to no more than 20 times the

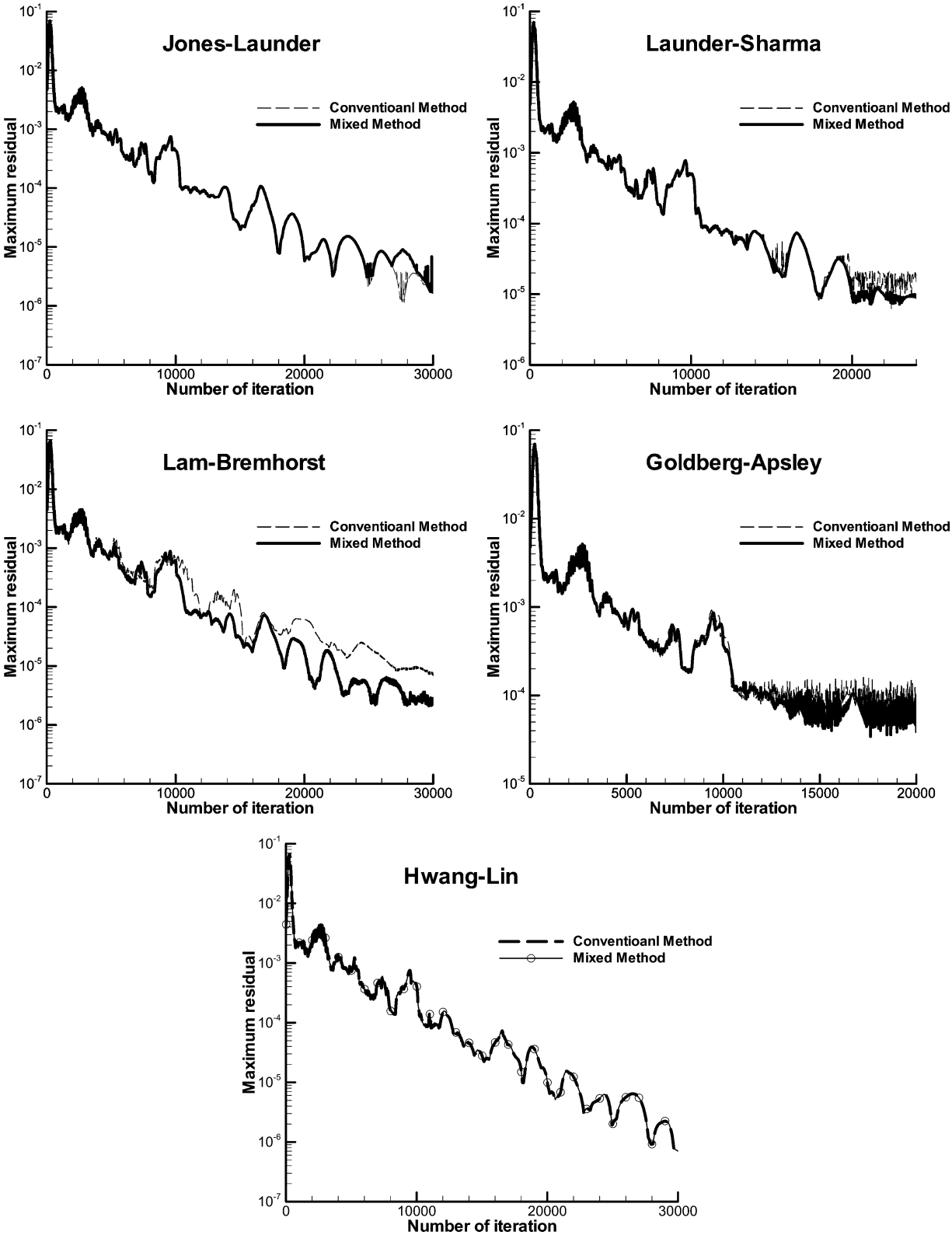

Fig. 8 Convergence history for RAE2822: mixed method and traditional method.

dissipation term. We use the same limiter as that in the conventional method in this paper accordingly.

Observe that in Eqs. (26) and (27), $\Psi_0 = (k_0/\varepsilon_0)\Phi$ appears in the denominator. This may cause trouble because Ψ_0 may vanish somewhere. To avoid this trouble, we set

$$B = G/(1/\rho)\Psi_0 = 1 + e^{2\mu\sqrt{\Phi}t} + \rho H(k_0/\varepsilon_0)2\mu t$$

where $H = [e^{2\mu\sqrt{(\Phi)}t} - 1]/[2\mu\sqrt{(\Phi)}t]$. Set

$$\lim_{2\mu\sqrt{\Phi}t \to 0} \left[(e^{2\mu\sqrt{\Phi}t} - 1)\Big/\left(2\mu\sqrt{\Phi}t\right)\right] = 1$$

hence, dividing by zero can be avoided by rewriting H as

$$H = \begin{cases} 1, & 2\mu\sqrt{\Phi}t < 10^{-4} \\ (e^{2\mu\sqrt{\Phi}t} - 1)\Big/\left(2\mu\sqrt{\Phi}t\right), & 2\mu\sqrt{\Phi}t > 10^{-4} \end{cases}$$

IV. Numerical Experiments

We use three test cases to assess the advantages of the mixed method: the transonic diffuser flow, RAE2822 flow, and NACA4412 flow.

A. Transonic Diffuser

1. Problem Definition

We consider transonic flow with a weak shock through a converging–diverging diffuser. The experiment was carried out by Sajben and Kroutil.[34] This configuration has an entrance-to-throat area ratio of 1.4, an exit-to-throat area ratio of 1.5, and a sidewall spacing of approximately four throat heights. Variation of the exit pressure leads to different shock positions and strengths. The corresponding Reynolds number is 9.370×10^5, and the Mach number is $M = 0.9$. The total pressure at inflow is 1.349×10^5 Pa, and the static pressure at the outflow is 1.11×10^5 Pa. These flows were characterized by the ratio R of exit static-to-inflow total pressure. For the weak-shock case, the value of R was 0.82.

2. Comparison Between the Mixed Method and the Conventional Method

Adiabatic no-slip boundary conditions were used on both the upper and lower walls. The inlet boundary conditions corresponded to uniform flow at $M = 0.9$. A constant static pressure was specified at the exit boundary.

The convergence history with the mixed method for various turbulent models is shown in Fig. 1, comparing that with traditional method. The CFL number is set to 1.0. We see that all computations with traditional methods fail to converge, whereas all models with the mixed method converge. The computation shows that the mixed analytical/numerical method can weaken the restriction of the time-step size and get convergence at larger time step. Of course, if a smaller CFL is considered, all models with the traditional method could also converge. In the computation by Barakos and Drikakis[35] with conventional method, the CFL number cannot exceed 0.3. In our computation with the conventional method and for the HL model, we see, from the convergence histories shown in Fig. 2, that the maximum allowable CFL number is 0.1.

The Mach contour with mixed the method for various turbulent models is shown in Fig. 3. All turbulent models give almost the same shock wave position. The static pressure distribution along the bottom and top walls are shown in Figs. 4 and 5, respectively, with comparison with the experimentally measured values. Figure 6 displays the velocity profiles at four axial locations $x/H = 2.882$, 4.611, 6.340, and 7.493 downstream of the shock wave. The agreement between computation and experiment is good.

3. Numerical Result with Implicit Residual Smoothing

To use a higher CFL number, we have included an implicit residual smoothing (IRS) to the mixed method that can be expressed as

$$\left(1 - \epsilon_x \delta_x^2\right)\left(1 - \epsilon_y \delta_y^2\right)\bar{R}(W) = R(W) \qquad (30)$$

Here, $R(W)$ and $\bar{R}(W)$ are the original and smoothed residuals, respectively, and ϵ_x and ϵ_y are the smoothing coefficients for the x and y directions, respectively.

The convergence histories are shown in Fig. 7. If the turbulent models are solved with the mixed method, the CFL number can be increased to two (JL and LS models) or even four (LB and HL models), whereas the computation diverges for the conventional method at the same CFL condition except for the LB model.

B. RAE2822 Airfoil

The RAE2822 airfoil has been used extensively for the validation of Navier–Stokes codes applied to transonic flow. This test problem is a benchmark problem used to verify the validation of turbulent model in Ref. 36. The flow conditions for this test case are freestream Mach number $M_\infty = 0.73$, Reynolds number $Re = 6.5 \times 10^6$, and angle of attack $\alpha = 3.19$ deg. The calculations were performed with a 369×65 grid provided by NASA.

Here, we use the RAE2822 test case to show advantage of the mixed method, notably to demonstrate that for large time steps, the solution while unstable at a given Δt with the conventional treatment is stable with the new treatment. We will also show that the mixed method does not increase the CPU time per iteration considerably.

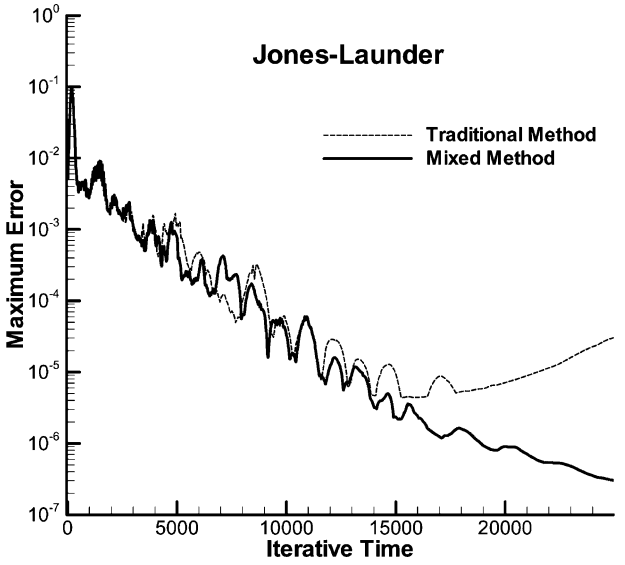

Fig. 9 Convergence history for RAE2822 with JS model: mixed method and traditional method (larger time steps).

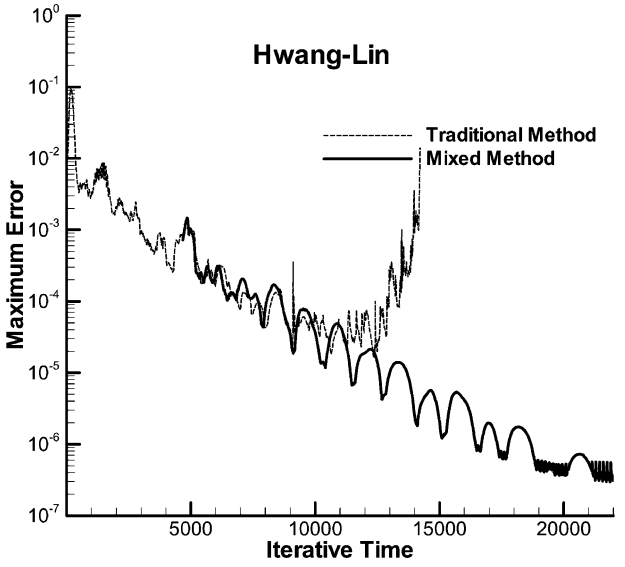

Fig. 10 Convergence history for RAE2822 with HL model: mixed method and traditional method (larger time steps).

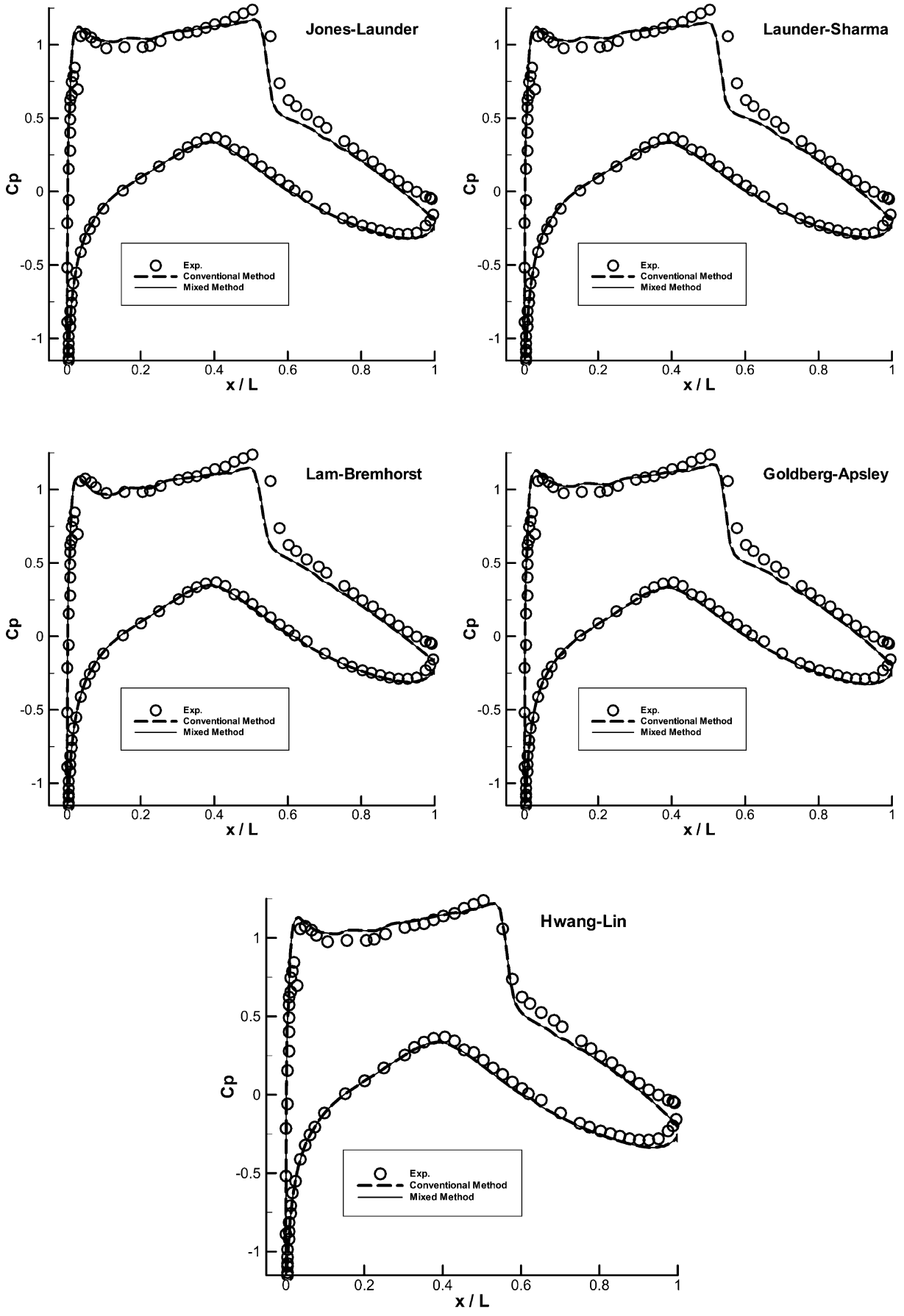

Fig. 11 Pressure coefficient profiles of RAE2822 airfoil with various turbulent models.

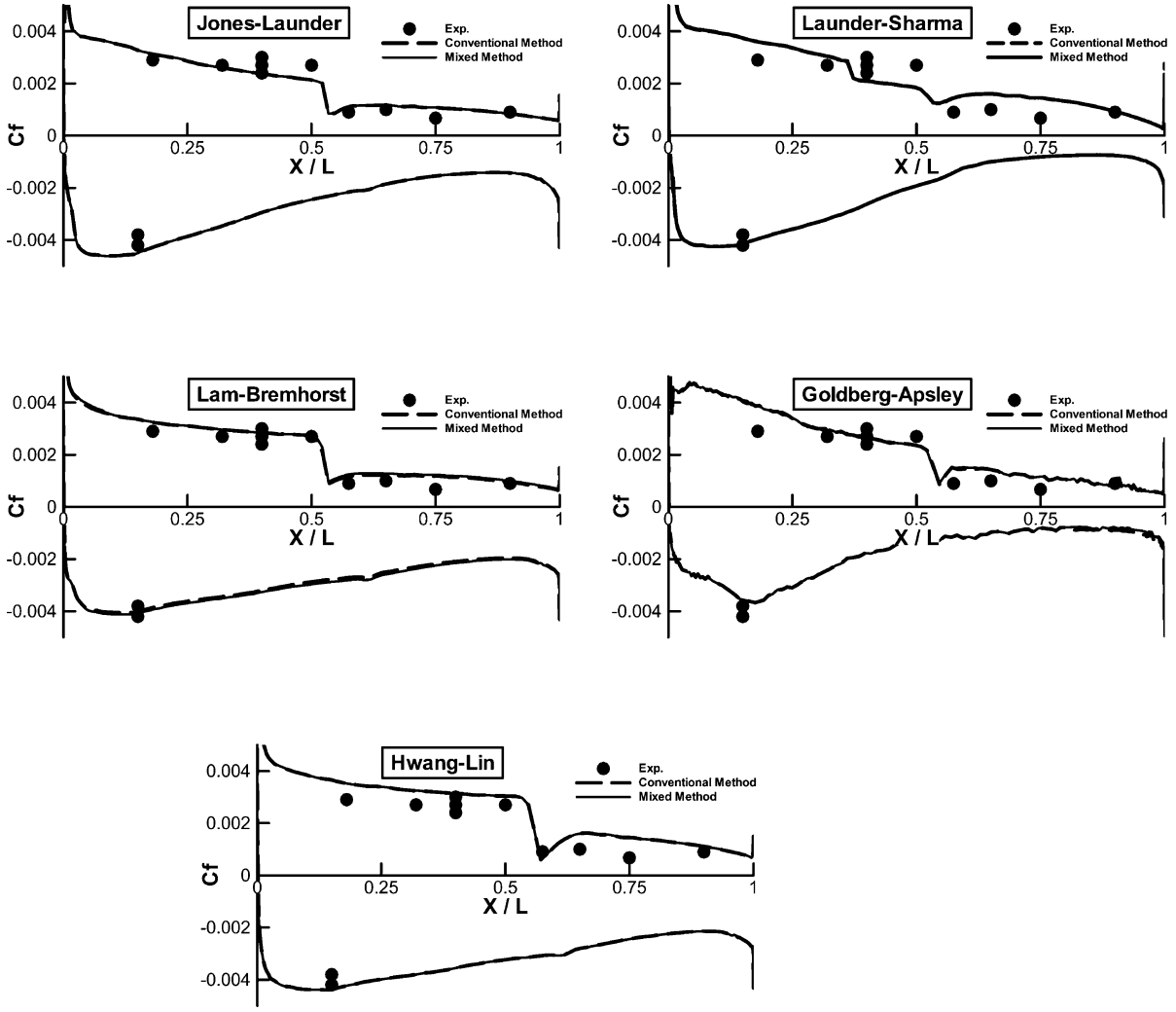

Fig. 12 Skin-friction coefficient profiles of RAE2822 airfoil with various turbulent models.

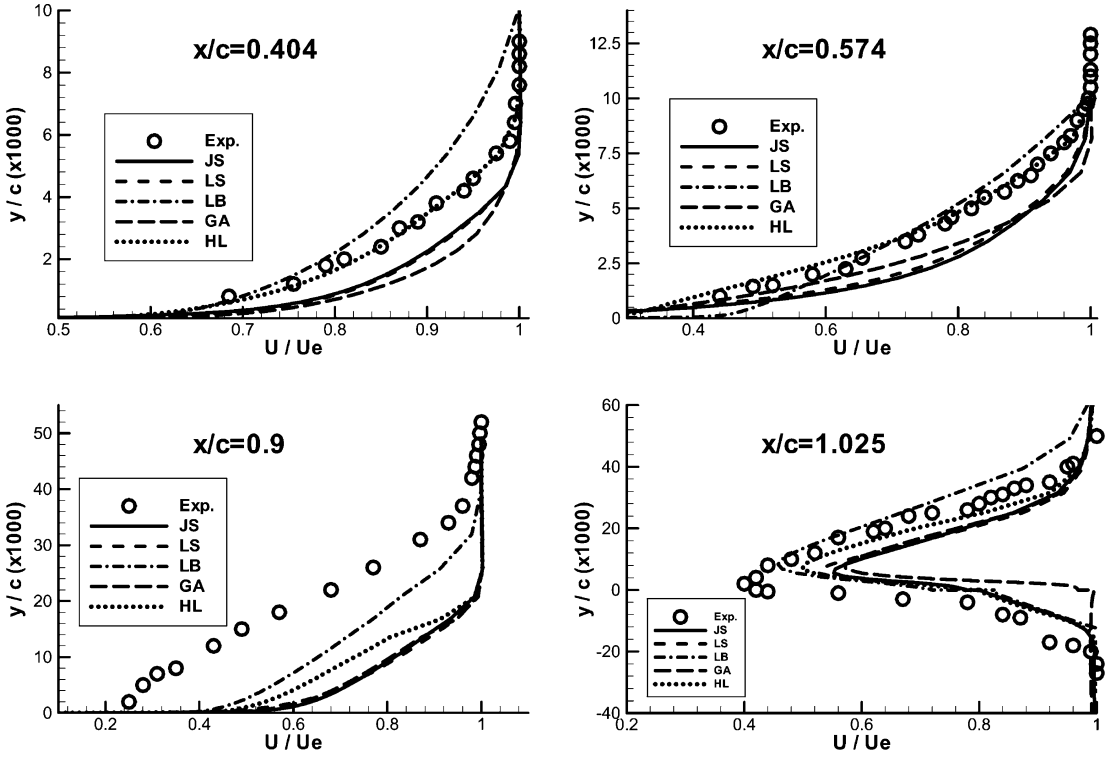

Fig. 13 Velocity profiles at four locations for the RAE2822 airfoil.

1. Comparison of the Convergence Speed

The convergence histories with the mixed method and the conventional numerical method for various turbulent models are displayed in Fig. 8. The CFL number is set to 0.5. For such a small time step, the mixed method, though slightly better than the conventional method, does not display a clear superiority in convergence speed.

Now, we use a larger time step by setting CFL = 1.0. The convergence histories with the mixed method and with the conventional numerical method for JL and HL turbulent models are displayed in Figs. 9 and 10, respectively. The computation is stable with the mixed method and unstable with the conventional method. Hence, larger time steps can be used with the mixed method, whereas the time step cannot exceed 0.5 for the conventional method.

Finally, we display the numerical solutions. The pressure coefficient and skin-friction coefficient obtained with the mixed methods, compared with experimental results, are shown in Figs. 11 and 12, respectively. Figure 13 shows the mean velocity profile with the mixed method compared with experimental data at four streamwise locations. Locations $x/c = 0.404$ and $x/c = 0.574$ are at the upstream of the shock wave, location $x/c = 0.90$ is at the downstream of the shock wave, and $x/c = 1.025$ is in the wake region.

2. Comparison of CPU Time

The number of work units consumed up to 800 iterations is shown in Table 4. Here, a work unit represents 1 min of CPU time on a Pentium III 550 microcomputer. Clearly, the mixed method is more expensive than the conventional method. The extra time is due to the analytical integration of the source term. Fortunately, this extra time does not exceed 15% of the total CPU time. This is negligibly small in comparison with the advantage of the mixed method.

C. NACA4412 Airfoil

In this test case, the angle of attack is $\alpha = 3.19$ deg. The Reynolds number is 1.52×10^6, and freestream Mach number $M_\infty = 0.2$. For this condition, a steady trailing-edge separation occurs.[37] Transition occurs at about 2% of the chord length. Numerical tests have shown that the transition location has little influence, as long as it is far enough upstream to prevent laminar separation. In this paper, the transition is considered. The production term in the transport

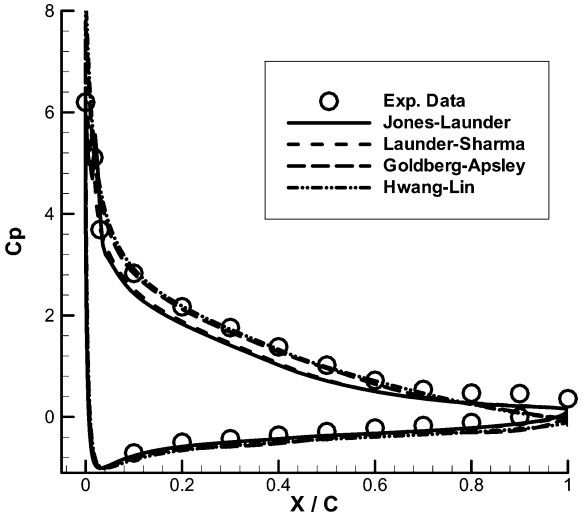

Fig. 15 Pressure coefficient profiles of NACA4412 airfoil with mixed method for various turbulent model.

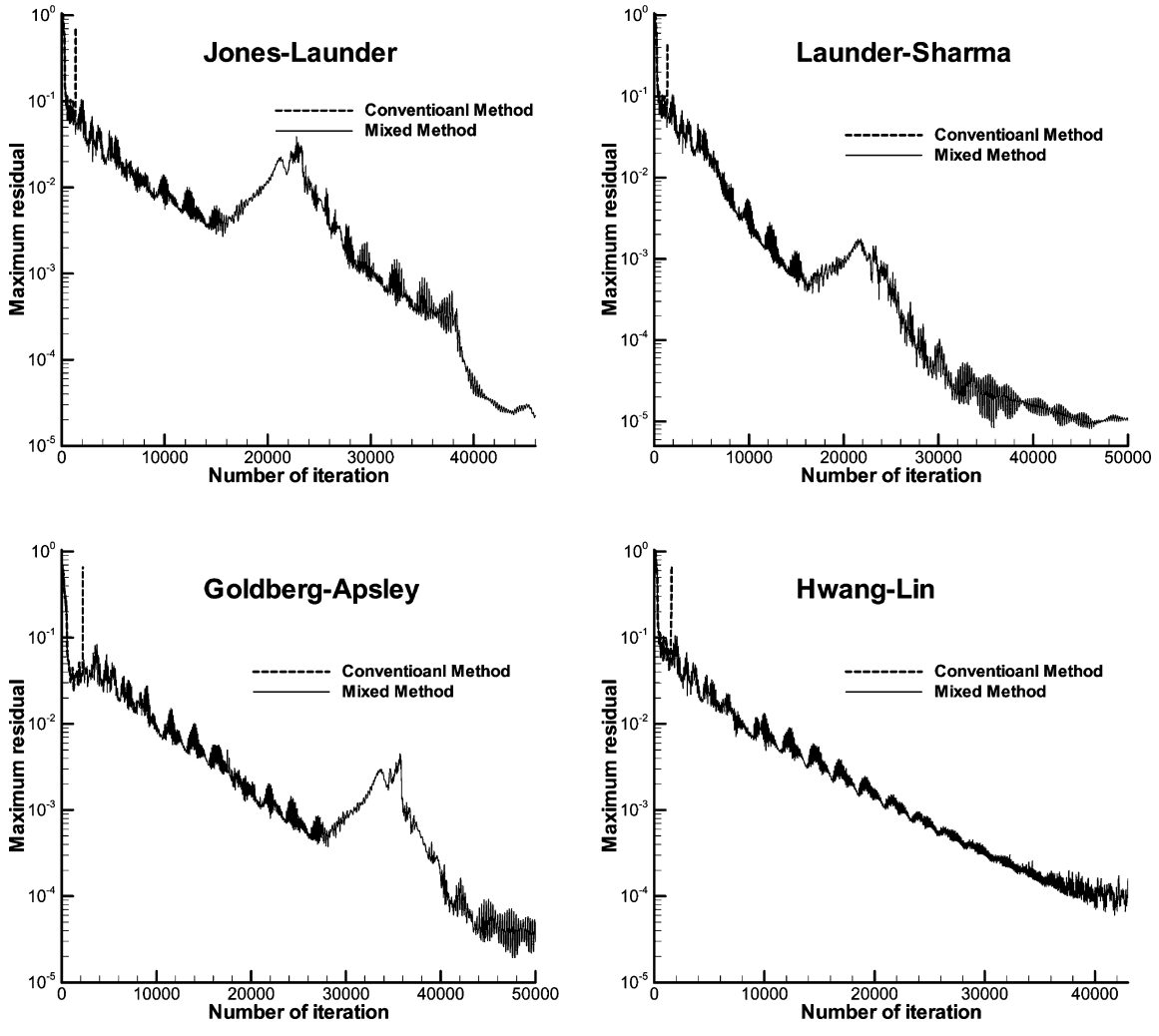

Fig. 14 Convergence history for NACA4412: mixed method and traditional method.

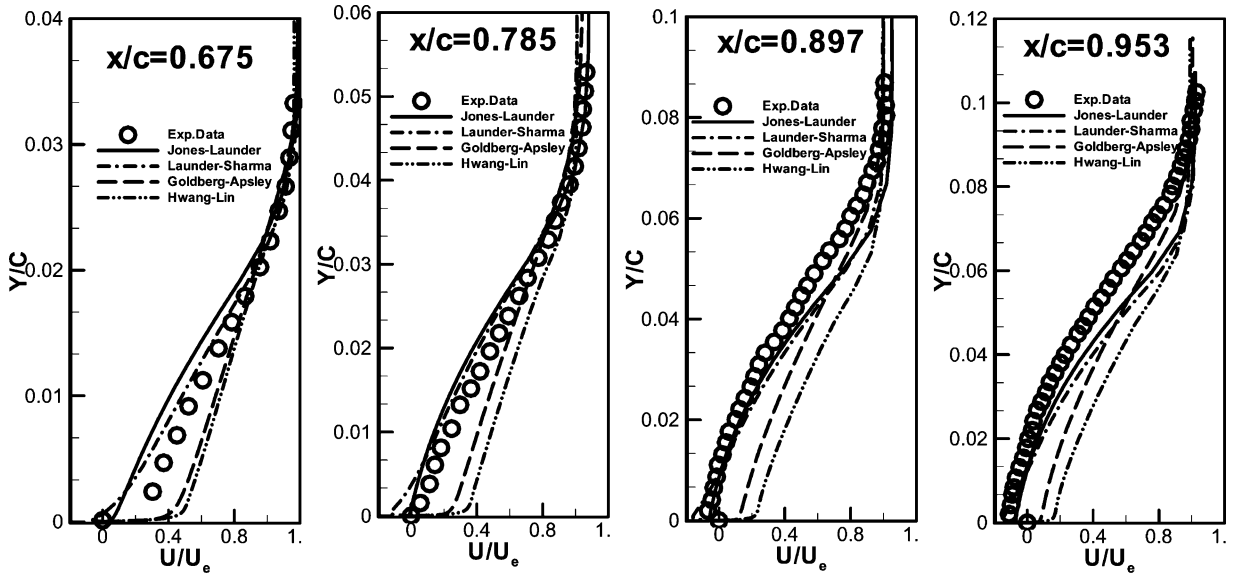

Fig. 16 Velocity profiles at four locations for the NACA4412 airfoil.

Table 4 Work units comparsion between mixed and conventional method at 800 iterations for RAE2822

Model	Conventional method T_t	Mixed method T_m	$(T_m - T_t)/T_t \times 100\%$
LS	56.2	60.6	8%
HL	53.3	60.3	13%

equation for the turbulent kinetic energy is set to zero upstream of these locations to represent transition effects. A 265×81 computational grid is used.

The convergence histories with the mixed method and with the conventional numerical method computed with CFL = 1.0 are displayed in Fig. 14. The computation is stable with the mixed method, whereas it is unstable with the conventional method. The pressure coefficient profiles computed with the mixed method are displayed in Fig. 15. The velocity profile is shown in Fig. 16. The HL model gives the best pressure coefficient distribution. The JS model and LS model with Yap correction give the trailing-edge separation. These models fail to represent the velocity profiles accurately in the zone with strong adverse pressure gradient. This shortcoming was attributed by Menter[33] to the definition of the eddy viscosity.

V. Conclusions

In this paper, we have built a mixed analytical/numerical method for the numerical solutions of low-Reynolds-number k–ε turbulence models. In this method, the advection–diffusion part of the turbulence models is solved by any traditional numerical method. We used the second-order Roe scheme for the inviscid part of the Navier–Stokes equations and the second-order central difference scheme for the viscous part. The source term is split into two parts, the first part is similar to the source term of a high-Reynolds-number model modified by damping factors and the second part takes into account the additional terms. The second part is integrated in time, as is the advection–diffusion part, and the first part is integrated analytically by freezing the damping factors as constant at each time step.

Three test cases have been used to assess the advantage of the mixed method over a traditional treatment. These are a transonic diffuser flow, an RAE2822 flow, and a NACA4412 flow. All are standard test cases. Various low-Reynolds-number models have been considered.

From the numerical results, we can draw the following conclusions:

1) When the same time step is used, the mixed method converges faster than the conventional pure numerical method.

2) For large times steps the solution, although unstable at a given Δt with the conventional treatment is stable with the new treatment. This means that the mixed method allows for the use of larger time steps.

3) The mixed method is slightly more expensive than the traditional method, but the overhead, which is due to the analytical integration of the source terms, only represents a small fraction (close to 10%) of the total CPU time.

Acknowledgments

This work has been supported by the China NKBRSF Project (2001CB409600) and the National Natural Science Foundation of China (10025210). The authors are grateful to the referees for their valuable comments with regard to this paper.

References

[1]Launder, B. E., "Numerical Computation of Convective Heat Transfer in Complex Turbulent Flow: Time to Abandon Wall Function?," *International Journal of Heat and Mass Transfer*, Vol. 27, No. 9, 1984, pp. 1485–1491.

[2]Jones, W. P., and Launder, B. E., "The Calculation of Low-Reynolds-Number Phenomena with a Two-Equation Model of Turbulence," *International Journal of Heat and Mass Transfer*, Vol. 16, 1974, pp. 1119–1130.

[3]Launder, B. E., and Sharma, B. I., "Application of the Energy Dissipation Model of Turbulence to the Calculation of Flow Near a Spinning Disc," *Letters in Heat and Mass Transfer*, Vol. 1, No. 2, 1974, pp. 131–138.

[4]Goldberg, U., and Apsley, D., "A Wall-Distance-Free Low Re k–ε Turbulence Model," *Computer Methods in Applied Mechanics and Engineering*, Vol. 145, 1997, pp. 227–238.

[5]Hwang, C. B., and Lin, C. A., "Improved Low-Reynolds-Number Model Based on Direct Numerical Simulation Data," *AIAA Journal*, Vol. 36, No. 1, 1998, pp. 38–43.

[6]Johnson, R. W., *The Handbook of Fluid Dynamics*, CRC Press, Boca Raton, FL, 1998, Chap. 14.

[7]Mohammadi, B., and Pironneau, O., *Analysis of the K–Epsilon Turbulence Model*, Wiley Masson, New York, 1994.

[8]Wu, Z. N., and Fu, S., "Positivity of k–Epsilon Turbulence Models for Incompressible Flow," *Mathematical Model and Methods in Applied Science*, Vol. 12, No. 3, 2002, pp. 393–406.

[9]Lew, A. J., Buscaglia, G. C., and Carrica, P. M. A., "Note on the Numerical Treatment of the k–Epsilon Turbulence Model," *International Journal of Computational Fluid Dynamics*, Vol. 14, 2001, pp. 201–209.

[10]Zhao, Y., "Stable Computation of Turbulent Flow with a Low-Reynolds-Number K–ε Turbulence Model and Explicit Solver," *Advances in Engineering Software*, Vol. 28, 1997, pp. 487–499.

[11]Mavriplis, D. J., and Martinelli, L., "Multigrid Solution of Compressible Turbulent Flow on Unstructured Meshes Using a Two-Equation Model," *International Journal for Numerical Method in Fluids*, Vol. 18, 1994, pp. 887–914.

[12]Vandromme, D., and Ha Minh, H., "About the Coupling of Turbulence Closure Models with Averaged Navier–Stokes Equations," *Journal of Computational Physics*, Vol. 65, No. 2, 1986, pp. 384–409.

[13]Sahu, J., and Danberg, J. E., "Navier–Stokes Computations of Transonic Flows with a Two-Equation Turbulence Model," *AIAA Journal*, Vol. 24, 1991, pp. 1744–1751.

[14]Shih, T. I.-P., and Chyu, W. J., "Approximate Factorization with Source Terms," *AIAA Journal*, Vol. 29, No. 10, 1991, pp. 1759–1760.

[15]Huang, P. G., and Coakley, T. J., "An Implicit Navier–Stokes Code for Turbulent Flow Modeling," AIAA Paper 92-0547, 1992.

[16]Merci, B., Steelant, J., Vierendeels, J., Riemslagh, K., and Dick, E., "Computational Treatment of Source Terms in Two-Equation Turbulence Models," *AIAA Journal*, Vol. 38, No. 11, 2000, pp. 2085–2093.

[17]Kunz, R. F., and Lakshminarayana, B., "Stability of Explicit Navier–Stokes Procedures Using k–ε and k–ε/Algebraic Reynolds Stress Turbulence Models," *Journal of Computational Physics*, Vol. 103, 1992, pp. 141–159.

[18]Bermudez, L., and Vazquez, M. E., "Upwind Methods for Hyperbolic Conservation Laws with Source Terms," *Computers and Fluids*, Vol. 23, 1994, pp. 1049–1071.

[19]Jin, S., and Xin, Z. P., "The Relaxation Schemes for Systems of Conservation Laws in Arbitrary Space Dimensions," *Communications on Pure and Applied Mathematics*, Vol. 48, 1995, pp. 235–276.

[20]Greenberg, J. M., and Le Roux, A.-Y., "A Well-Balanced Scheme for the Numerical Processing of Source Terms in Hyperbolic Equations," *SIAM Journal on Numerical Analysis*, Vol. 33, 1996, pp. 1–16.

[21]Bao, W. Z., and Jin, S., "The Random Projection Method for Hyperbolic Conservation Laws with Stiff Reaction Terms," *Journal of Computational Physics*, Vol. 163, 2000, pp. 216–248.

[22]Helzel, C., LeVeque, R. J., and Warnecke, G., "A Modified Fractional Step Method for the Accurate Approximation of Detonation Waves," *SIAM Journal on Scientific Computing*, Vol. 22, 2000, pp. 1489–1510.

[23]Du, T., Shi, J., and Wu, Z. N., "Mixed Analytical/Numerical Method for Flow Equations with a Source Term," *Computers and Fluids*, Vol. 32, 2003, pp. 659–690.

[24]Du, T., and Wu, Z. N., "Mixed Analytical/Numerical Method Applied to the High Reynolds Number k–ε Turbulence Model," *Computers and Fluids* (to be published).

[25]Lam, C. K. G., and Bremhorst, K. A., "A Modified Form of the k–ε Model for Predicting Wall Turbulence," *Journal of Fluids Engineering*, Vol. 103, 1981, pp. 456–459.

[26]Yap, C. R., "Turbulent Heat and Momentum Transfer in Recirculating and Impinging Flows," Ph.D. Dissertation, Dept. of Mechanical Engineering, Faculty of Technology, UMIST, Manchester, England, U.K., 1987.

[27]Jameson, A., "Transonic Flow Calculations," Mechanical and Aerospace Engineering, MAE Rept. 1651, Princeton Univ., Princeton, NJ, 1983.

[28]Roe, P. L., "Approximate Riemann Solvers, Parameter Vectors, and Difference Schemes," *Journal of Computational Physics*, Vol. 43, 1981, pp. 357–372.

[29]van Leer, B., "Towards the Ultimate Conservative Difference Scheme. V. A Second-Order Sequel to Godunov's Method," *Journal of Computational Physics*, Vol. 32, 1979, pp. 101–136.

[30]Anderson, W. K., Thomas, J. L., and van Leer, B., "Comparison of Finite Volume Flux Vector Splitting for the Euler Equations," *AIAA Journal*, Vol. 24, 1986, pp. 1453–1460.

[31]Steelant, J., and Dick, E., "A Multigrid Method for the Compressible Navier–Stokes Equations Coupled to the k–ε Turbulence Equations," *International Journal of Numerical Methods in Heat and Fluid Flow*, Vol. 4, No. l2, 1994, pp. 99–113.

[32]Kral, L. D., "Recent Experience with Different Turbulence Models Applied to the Calculation of Flow over Aircraft Components," *Progress in Aerospace Sciences*, Vol. 34, 1998, pp. 481–541.

[33]Menter, F. R., "Two-Equation Eddy–Viscosity Turbulence Models for Engineering Applications," *AIAA Journal*, Vol. 32, 1994, pp. 1598–1605.

[34]Sajben, M., and Kroutil, J. C., "Effects of Initial Boundary-Layer Thickness on Transonic Diffuser Flows," *AIAA Journal*, Vol. 19, No. 11, 1981, pp. 1386–1393.

[35]Barakos, G., and Drikakis, D., "Assessment of Various Low-Reynolds Number Turbulence Models in Shock–Boundary Layer Interaction," *Computer Methods in Applied Mechanics and Engineering*, Vol. 160, 1998, pp. 155–174.

[36]Kline, S. J., Cantwell, B. J., and Lilley, G. M., *U.S. Air Force Office of Scientific Research, AFOSR–HTTM—Stanford Conference on Complex Turbulent Flows*, Stanford Univ., Stanford, CA, 1981.

[37]Coles, D., and Wadcock, A. J., "Flying-Hot-Wire Study of Flow Past a NACA4412 Airfoil at Maximum Lift," *AIAA Journal*, Vol. 17, 1979, pp. 321–329.

W. Devenport
Associate Editor